A statistical multi-scale approach to evaluate the risk of infection by respiratory droplets

L Campanelli[1,*], P Tartarini[2] and M Cavazzuti[1]

[1] Dipartimento di Scienze e Metodi dell'Ingegneria, Università degli Studi di Modena e Reggio Emilia, via Giovanni Amendola 2, Reggio Emilia, 42122, Italia

[2] Dipartimento di Ingegneria "Enzo Ferrari", Università degli Studi di Modena e Reggio Emilia, via Pietro Vivarelli 10, Modena, 41125, Italia

[*] Corresponding author: ludovico.campanelli@unimore.it

Abstract. Predicting the dispersion of respiratory droplets deterministically is an exceedingly challenging task due to the substantial number of variables affecting the droplet trajectory and evaporation. For this reason, statistical models are recommended to obtain potential ranges for the quantities of interest. Recently, the authors have developed an analytical model that evaluates droplet trajectory and evaporation rate; through randomisation elements, the model can perform also statistical analysis on droplet dispersion. Although elaborated, the analytical model has limits for what concerns its predictive capability over intrinsically three-dimensional fluid dynamics features such as the dynamics of the unsteady exhaled breath cloud and the effect of turbulence. In this framework it is of interest to couple the analytical model developed to unsteady 3D CFD simulations of the exhaled airflow, thus replacing the empirical model of the jet and overcoming the modelling limits. In this work, a one-way coupling method is proposed, in which the analytical model reads the local velocity and thermohygrometric conditions from the CFD results and computes the droplet trajectory and evaporation rate accordingly. Finally, a statistical analysis is performed to compare the two models and to assess the reliability of the initial analytical model which, although simplified, provides a much more flexible approach.

1. Introduction

In recent years there has been a growing interest towards the development of models aiming at predicting the risk of infectious disease transmission by respiratory droplets.

These models are important as they can support the choice of proper guidelines for mitigating the pathogen spread, such as those related to social distancing measures. During respiratory events (such as breathing, speaking, coughing, and sneezing) droplet of different sizes are released, whose diameter can range from a millimetre down to a fraction of micrometre. Depending on their size and local thermohygrometric conditions, exhaled droplets have a different fate: larger ones follow a parabolic path driven by gravity while smaller ones are mainly transported by the local air flow until they settle on a surface or are inhaled by a susceptible host. Another important aspect is the difference in terms of vapour partial pressure between the droplet surface and the surroundings driving the evaporation of the droplet's liquid fraction. This suggests that the volume of the particles is not constant, but decreases until the droplet, eventually, becomes airborne, after having dried out and only its solid fraction remains. Airborne

particles can be carried arbitrarily far by the local air flow, and the pathogens contained can survive up several days.

In the literature there are several approaches to model this kind of problem, many authors used CFD to model respiratory events for different scenarios. Borro *et al.* [1] performed Eulerian-Lagrangian simulations to model the droplet dispersion from a cough in a hospital room for different ventilation strategies. It was found that doubling the HVAC airflow results in a greater reduction of contaminant concentration and the use of Local Exhaust Ventilation for the infected individual can avoid the infection of the healthcare personnel. CFD models have a great capability in capturing airflow features, nonetheless the results are valid only for the scenario modelled and cannot be generalised easily (i.e. any change in the geometry can alter the airflow pattern significantly). Another approach found in the literature is the use of analytical models, to solve the droplet governing equations. Balachandar *et al.* [2] developed a two-dimensional analytical model to evaluate droplet dispersion and evaporation rate where the exhaled jet is modelled as an non-isothermal unsteady jet derived from the momentum conservation hypothesis. Momentum dissipation due to the drag is accounted for to better represent the actual phenomena. Generally, analytical models can provide a good accuracy with a lower computational effort compared to CFD based models, but they have limits on the prediction of three dimensional features.

The authors have developed an analytical model [3] that implements the governing equations of droplet transport, energy balance, evaporation, and chemical species. The unsteady jet exhaled from the mouth (or from the nostrils) is modelled empirically, and a discrete random walk approach is implemented to mimic the effect of turbulent dispersion on the local droplet trajectories. To allow stochastic analyses to be performed, additional features were implemented such as the randomisation of the initial droplet position on the inlet surface and of the droplet injection time within the exhalation time span of the respiratory event being modelled. In this work a statistical analysis performed with a multi-scale model is presented, where the empirical formulation for the breath cloud is replaced by an unsteady CFD simulation of the respiratory event under investigation. In this way it is possible to include intrinsic aspects of the 3D simulation that cannot be modelled empirically. From the analysis, risk maps are obtained to asses the infection risk in indoor environments. The results are then compared with those of the original analytical model.

2. Analytical model

In this section the equations used to predict the droplet transport, evaporation rate and temperature are briefly recalled. A more comprehensive discussion on the self-developed analytical model can be find in a previous work by the authors [3].

After the ejection, the droplet can be considered in free fall, hence the main forces that govern its trajectory are its weight and drag, while other forces are assumed negligible [4]. From Newton's second law of motion, the droplet velocity vector $\mathbf{u}_\mathrm{p}(t)$ is obtained by integrating the acceleration with the initial condition $\mathbf{u}_\mathrm{r}(0) = \mathbf{u}_{\mathrm{r},0}$

$$\mathbf{u}_\mathrm{p}(t) = \mathbf{u}_\mathrm{m,s} + \mathbf{u}_{\mathrm{r},0} e^{-t/\tau_\mathrm{d}} + \mathbf{u}_{\mathrm{r},t} \frac{\tau_\mathrm{d}}{\tau_{\mathrm{d},t}} \left(1 - e^{-t/\tau_\mathrm{d}} \right) \quad , \tag{1}$$

where $\mathbf{u}_\mathrm{r}$=$\mathbf{u}_\mathrm{p}$−$\mathbf{u}_\infty$ is the relative velocity vector between the droplet and the local undisturbed air flow, and τ_d is the drag characteristic time. Subscript "p" refers to the droplet,"m,s" to the humid air mixture by the droplet surface, and "t" denotes the terminal condition, namely the condition at infinite time, when $\mathbf{u}_\mathrm{r}$=0. From the equation (1) it can be noted that for small terminal velocity and high timespan the droplet velocity is equal to that of surrounding air, as such it can be transported arbitrarily far from the emitter.

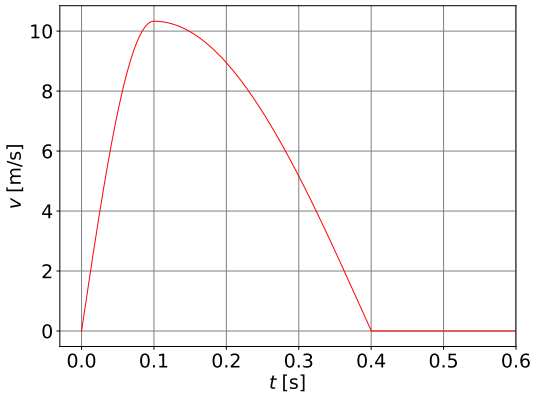


Figure 1. Coughing velocity.

The mass transfer from the droplet surface to the ambient is modelled by means of the stationary convection-diffusion equation, without source term and neglecting cross diffusion of air in water. After some mathematical manipulations and by integrating the equation in time, the diameter reduction with the time can be written as

$$D_{\mathrm{p}}(t) = \sqrt{D_{\mathrm{p},0}^2 - Kt}\,, \tag{2}$$

where K is the evaporation rate and $D_{\mathrm{p},0}$ the initial size.

The sensible thermal power stored by the droplet is balanced by evaporative cooling and convective heating

$$\dot{Q}_{\mathrm{sn}} = \dot{Q}_{\mathrm{ev}} + \dot{Q}_{\mathrm{cv}}\,. \tag{3}$$

Equation (3) can be rewritten in terms of droplet temperature rate of change and by integrating with an initial droplet temperature $T_{\mathrm{s},0}$, the equation for the droplet temperature is derived

$$T_{\mathrm{p}}(t) = T_{\mathrm{s},0}\mathrm{e}^{-t/\tau_{\mathrm{ev}}} + T_{\mathrm{s,t}}(1 - \mathrm{e}^{-t/\tau_{\mathrm{ev}}}) \tag{4}$$

where τ_{ev} is the characteristic time associated to evaporation and $T_{\mathrm{s,t}}$ is the droplet terminal temperature.

3. Methods

The analytical model recalled in the previous section also includes an empirical model for the buoyant unsteady jet emitted during the respiratory event.

The analytical modelling of the emitted jet is a challenging task, due to its unsteady and three-dimensional nature. In this context, unsteady CFD simulations have a major advantage over analytical models, at the cost of a larger computational demand. In this work, the unsteady jet is simulated with a 3D CFD model which is then coupled to the analytical model in place of the empirical one; the methodology used for the one-way coupling is described in a previous work by the authors [5] where preliminary results are shown for a 2D case study. The present paper extends the aforementioned work with the addition of 3D modelling, randomisation of the droplet release and random walk model (described in [3]) to mimic the particle's turbulent dispersion.

3.1. Case study

This work investigates the infection risk due to a cough by an infected individual in a quiescent air environment.

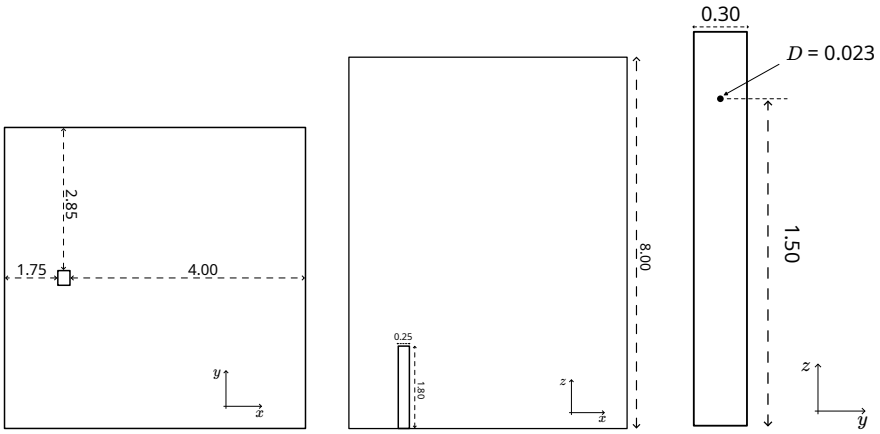


Figure 2. CFD model geometry: (a) top view, (b) side view, (c) mannequin front view. Measures are in meters.

Table 1. Boundary and initial conditions used in the CFD simulation.

Patch	**Velocity**	***T***	***RH***
walls	no-slip	adiabatic	zero-gradient
mannequin	no-slip	301.15 K	zero-gradient
mouth	velocity coughing function (see figure 1)	307.15 K	95 %
internalField	zero velocity	293.15 K	50 %

According to the work by Gupta *et al* [6], the flow accelerates in the first 0.12 s and then decelerates until it reaches zero velocity after 0.40 s from the start. The total exhaled volume is assumed to be 1 l, with an average flow rate of 2.5 l/s and a peak velocity of 10.3 m/s. The mouth diameter is 0.022 m and the jet inclination is assumed to be $-27.5°$. Figure 1 shows the velocity variation in time at the mouth cross section during the coughing event. Regarding the released droplet sizes, different distributions are proposed in the literature. As suggested in [2], the distribution that better fits the data in the literature is a power law Probability Density Function $\mathcal{B}(D_p) = B/D_p^m$, where m and B are constants to be determined. In the following $m = 2$ has been chosen [2] and, by averaging the data provided in the review by Bourouiba [7], the coefficient $B = 2 \times 10^{-2}$ m/s is assumed for D_p in the range $10^{-1} - 10^3$ µm.

3.2. CFD model

Figure 2 shows the geometry of the CFD model, which consists of a mannequin representing an infected individual in a 6 m × 6 m × 8 m room.

To minimise the effect of boundaries, the walls are placed at a sufficient distance from the mannequin's mouth, which is at a height of 1.5 m above the floor. A custom OpenFOAM solver was used for the simulation [8], which works as the classic single-phase heat transfer solver provided by OpenFOAM, but can model humid air. The simulation was performed using the *k-ω SST* turbulence model. Table 1 summarises boundary and initial conditions. At the walls no slip and adiabatic conditions are enforced. To model the thermal plume by the body, the mannequin temperature is set to $28°C$. The transient velocity function in figure 1 is imposed on the mouth surface with a temperature of $34°C$. The initial conditions for the internal cells are

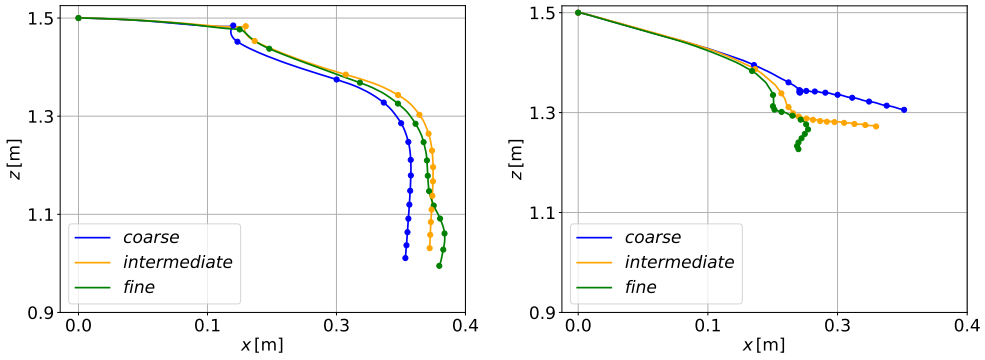


Figure 3. Grid sensitivity analysis. Trajectory of a 100 µm (a) and 10 µm (b) droplet on the $x - z$ plane. Dots are traced at 0.1 s intervals.

Table 2. Mesh sensitivity test.

Grid	**Elements** [$\times 10^4$]	$\boldsymbol{l_{min-avg}}$ [m]	$\boldsymbol{\bar{d}_{100}}$ [mm]	$\boldsymbol{\bar{d}_{10}}$ [mm]
Coarse	25	$0.0011 - 0.15$	22.84	60.90
Intermediate	85	$0.00070 - 0.11$	18.90	30.92
Fine	336	$0.00019 - 0.070$	–	–

zero velocity and a temperature of $20°C$ with relative humidity of 50 %. The relative humidity at the mouth is set to 95 %, while in all the other boundaries zero humidity gradient is imposed.

The computational grid is hybrid with both structured and unstructured elements. Cell size is finer close to the mannequin while getting coarse with the distance from the emitter. The grid sensitivity analysis focuses on two coupled simulation of a 100 µm and a 10 µm droplet, where the turbulent dispersion has been turned off. The droplets are ejected at time 0.1 s, i.e. when the coughing velocity reaches its peak, and the simulation stops at 1.5 s. Figure 3 shows the droplet trajectories in the $x - z$ plane obtained with 3 different grids. The 100 µm droplet (figure 3a) is falling mostly driven by gravity, while the 10 µm droplet (figure 3b) is transported by the local airflow, as such its trajectory is most influenced by grid refinement. The dots in the plots point out the droplet position at time intervals of 0.1 s. Table 2 resumes the results of the mesh sensitivity analysis. The second column reports the number of elements of the grids, while the third column shows the minimum and average cell diagonal size. The fourth and fifth columns show the average Euclidean distance $\bar{d}$ with respect to the result of the fine grid for the two droplets measured at time intervals of 0.1 s. As expected, the 10 µm particle presents the largest distances; being 60.90 mm for the coarse mesh, and 30.92 mm for the intermediate grid. Although the average distances are not particularly small, they are considered acceptable for the statistical analysis performed. The intermediate mesh is chosen as the best compromise solution between the required accuracy and computational resources needed for the simulation.

The simulation time-step is adaptive, and is chosen so that the maximum Courant number does not exceed unity. The solution is saved every 0.02 s.

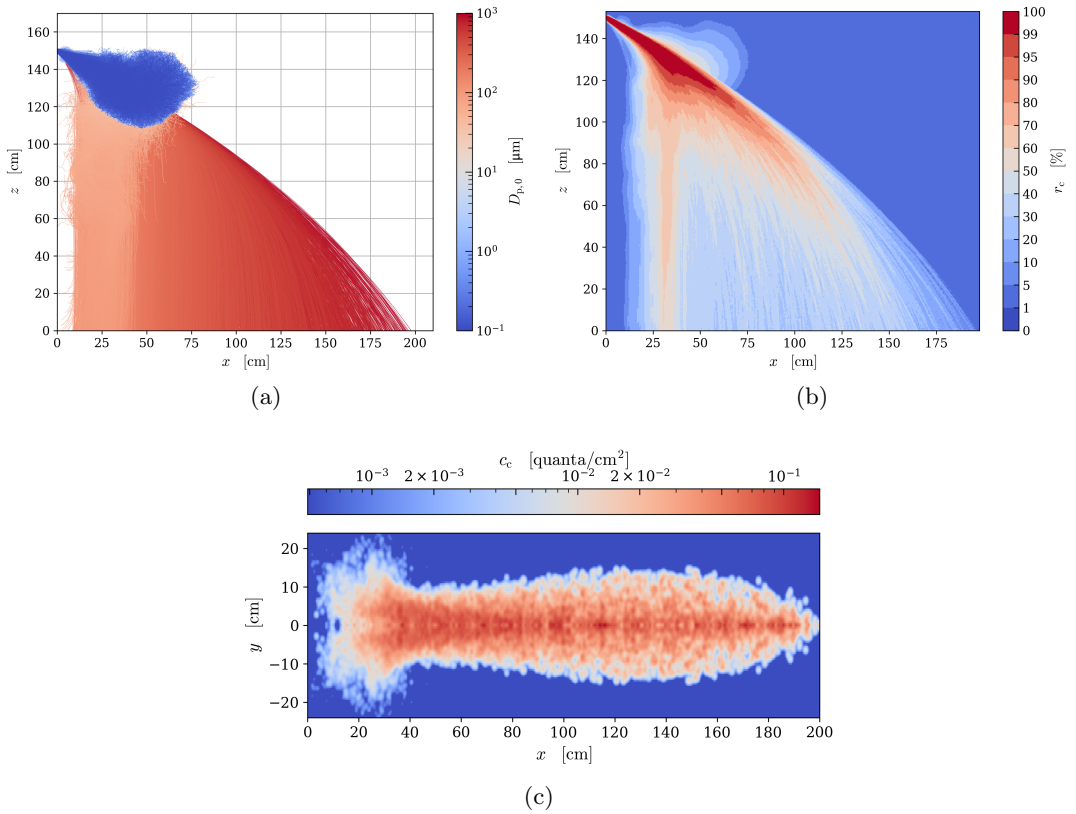


Figure 4. Simulation results using the multi-scale model: a) droplet trajectories, b) infection risk map, c) ground map.

4. Results

The described multi-scale model was used to perform a statistical analysis on droplet trajectory distribution. A set of 972 logarithmically distributed droplet diameters in the range $10^{-1} - 10^{3}$ µm has been simulated; the simulations are repeated 42 times for each diameter with the randomisation elements described above. Each simulation terminated when the particle reached the ground, or its relative velocity with respect to the local air is zeroed (i.e. the droplet is completely transported), or dried out. The trajectories are post-processed considering an average viral load in the saliva of 3.3 copies/nl, in line with the value suggested in [9] for SARS-CoV-2.

Figure 4a shows the trajectories of all simulated droplets, coloured by their initial diameter. As expected larger droplets ($D \gtrsim 100$ µm) follow a parabolic trajectory and reach the ground. Intermediate droplets ($20 \lesssim D \lesssim 100$ µm) remain airborne terminating the evaporation out of the breath cloud area of influence. Droplets with $D \lesssim 20$ µm are fully transported by the puff, and their trajectories are simulated until the breath cloud dissipates into the ambient air. Afterwards, they are assumed to be uniformly dispersed in the ambient air contributing to the background virus concentration in the room. Figure 4b is a risk map, derived from the previous trajectory distribution, based on the probability of inhaling suspended droplet nuclei. Being i_c the number of quanta inhaled by a susceptible individual breathing normally, where a quantum is the amount of viruses that cause infection in 63% of the susceptible host and is assumed equal to 100 virus copies in line with [10], the risk is evaluated as $r = 1 - e^{-i_c}$. The inhaled quanta are evaluated considering all the particles that cross the inhalation volume (assumed to be a hemisphere centred on the centre of each cell in the map) with a lower orthogonal velocity

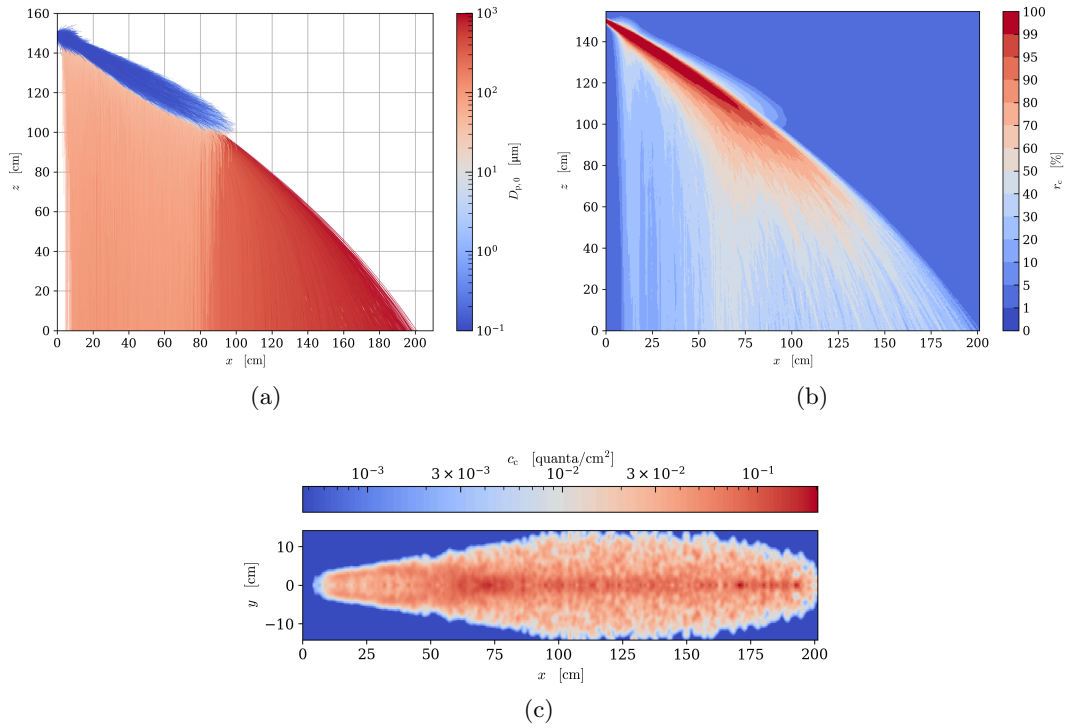


Figure 5. Simulation results using the analytical model: a) droplet trajectories, b) infection risk map, c) ground map.

compared to the local velocity of the air inhaled. For a more detailed explanation the reader is referred to [3]. From the map it can be noted that the risk of infection is nearly 100% close to the mouth, as almost all droplets cross that region. A risk greater than 60% is present along a vertical line at $x \simeq 30$ cm, where many of the mid-size droplets fall, and along the parabolic path followed by many large droplets. The risk inside the breath puff is not so high, since only small droplets, carrying a limited viral load, remain in the puff. Figure 4c depicts the virus quanta deposition rate on the ground per square centimetre. More than 90% of the exhaled quanta reach the ground, this is because the virus content is proportional to the droplet size. Larger droplets fall up to 2 metres far, while most particles reach a distance of about $1.2 - 1.5$ metres. Close to the emitter the quanta concentration on the ground is lower since in that region only the smallest droplets, among those reaching the ground, being more damped by drag, fall. Figure 5 shows the same results obtained with the original analytical model. From figure 5a it can be noted how the empirical cloud model is characterised by a greater outreach compared to the coupled model. Further, the spread of the puff is smaller. This difference is due to the greater turbulent dispersion inherent to the CFD results. Another significant difference is in the trajectory of the mid-size particles leaving the cloud because of gravity; in the original analytical model these particles fall vertically along the entire cloud extension, whereas in the coupled model they are deflected towards the emitter by the vortices generated at the breath cloud shear layer. This particular behaviour cannot be caught by the empirical cloud model, that assumes quiescent air outside of the puff. This leads to a different distribution of the infection risk, in fact in figure 4b the risk is greater in the area where most of the intermediate droplets are deflected by the shear layers vortices, while in figure 5b the droplets are more evenly distributed and the risk is milder. In addition, the different shape of the breath cloud between the two models, results in a different risk associated with the cloud area itself. The ground concentration map obtained with the original analytical model is shown in figure 5c. This is very similar to figure

4c, except for a lower spread near to the emitter. Despite these discussed differences, the two models, are in good agreement both in qualitative and quantitative terms. The dissimilarities are mostly due to the higher droplet dispersion in the coupled model. The maximum falling distance is approximately 2 m for both models. From figure 4a and figure 5a it can be seen that the trajectory of largest droplets is the same, as well as for the critical diameter below which the particles remain airborne. Regarding the risk maps, the two approaches leads to almost the same high risk region, except for the different shape of the breath cloud.

The results suggest that the simple analytical model is indeed suitable if the goal is that of assisting the development of improved safety measures.

5. Conclusions

In indoor environments, the transmission of pathogens from host to host occurs mainly through droplets exhaled during respiratory events. The development of appropriate preventive measures requires information about the droplet trajectories and the infection risk in the environment.

The authors have developed an analytical model to simulate droplet trajectory and evaporation under different boundary conditions. An empirical model of the buoyant exhaled jet based on momentum conservation hypothesis is implemented. Further, the randomisation of the droplet injection and a discrete random walk turbulent dispersion model enable statistical analyses on the droplet trajectory distribution, to be performed. The empirical model of the exhaled jet although elaborated, cannot capture the inherent 3D structures of turbulent jets. In this work, such empirical model is replaced by an unsteady 3D CFD simulation of the exhaled jet, which provides a more realistic representation of the buoyant breath cloud. The CFD and the analytical model are coupled using a one-way coupling method, where at each time step the analytical model obtains information about the local velocity and thermohygrometric conditions from the CFD results. The coupled model has been used to perform a statistical analysis of the infection risk caused by a coughing individual affected by SARS-CoV-2. The results are compared with those obtained from the original analytical model. The statistical analysis is performed on a set of over 41 thousand simulations. The results of the two models present some differences in the trajectory of the small droplets where gravity does not dominate over drag. These differences are mainly due to a greater droplet dispersion captured by CFD and inability of the original empirical breath cloud model to capture the jet shear layer. Larger droplet trajectories are driven by gravity and are little affected by the the local airflow. As a consequence the differences between the two models are minimal for what concerns these droplets. Since the virus content is proportional to the droplet size, the infection risk is mostly related to the fate of larger droplets.

As such, the analytical model has been demonstrated to be a flexible and reliable tool that can be used to obtain cheap and accurate information on the droplet trajectories and the associated risk of infection. On the other hand, the use of CFD simulations allows a more detailed analysis of small particles that are carried by the local airflow, at a higher computational cost.

6. References

[1] Borro L, Mazzei L, Raponi M, Piscitelli P, Miani A and Secinaro A 2021 *Environ Res* **193** 110343
[2] Balachandar S, Zaleski S, Soldati A, Ahmadi G and Bourouiba L 2020 *Int J Multiphas Flow* **132** 103439
[3] Cavazzuti M and Tartarini P 2023 *Phys Fluids* **35** 103327
[4] Elghobashi S and Truesdell G C 1992 *J Fluid Mech* **242** 655–700
[5] Campanelli L, Cavazzuti M and Tartarini P 2024 *J Phys: Conf Ser* **2685** 012066
[6] Gupta J K, Lin CH and Chen Q 2009 *Indoor Air* **19** 517-525
[7] Bourouiba L 2021 *Annu Rev Biomed Eng* **23** 547—577
[8] Holzmann T 2021, last access: 04/22/2024, url: https://github.com/shor-ty/humidityRhoThermo/
[9] Alsved M, Matamis A, Bohlin R, Richter M, Bengtsson P E, Fraenkel C J, Medstrand P and Löndahl J 2020 *Aerosol Sci Technol* **54** 1245–1248
[10] Kolinski J M and Schneider T M 2021 *Phys Rev E* **103** 033109